Pergamon

www.elsevier.com/locate/jappmathmech

PII: S0021-8928(02)00079-5

J. Appl. Maths Mechs, Vol. 66, No. 4, pp. 605–616, 2002
© 2002 Elsevier Science Ltd
All rights reserved. Printed in Great Britain
0021-8928/02/$—see front matter

THE AXISYMMETRIC POSTBUCKLING BEHAVIOUR OF SHALLOW SPHERICAL DOMES†

E. I. GRIGOLYUK and Ye. A. LOPANITSYN

Moscow

(*Received* 30 *January* 2001)

On the assumption that the buckling of an elastic, shallow spherical dome, rigidly clamped along a contour and loaded by a uniform transverse pressure, is finite and axisymmetric, its postbuckling behaviour is investigated. A solution is constructed based on the Marguerre equations using the Rayleigh–Ritz method with the displacements approximated by finite sums over Bessel functions. The system of non-linear algebraic equations obtained in this case is solved by the method of prolongation (the arc-length method). The effect of the wall-thinness parameter of the dome on its deformation curve is analysed. The phenomena of the generation of limit points in the loading trajectory, their merging and subsequent disappearance, as well as the phenomena of the joining of isolated loops to the main branch of the loading trajectory and of their detachment from it are discovered. The high sensitivity of the dome to deviations from an ideal shape is demonstrated. © 2002 Elsevier Science Ltd. All rights reserved.

Three stages are involved in the solution of the complete problem of the deformation of thin-walled structures under the action of static loads: the determination of the non-linear stress–strain state (SSS) of the structure until it lose stability, the solution of the problem of the stability of the structure when it has a prior, non-linear, stress–strain state and finding the possible unstable states of equilibrium of the structure after stability is lost with subsequent attainment of a stable, postbuckling, non-linear stress–strain state.

The publication of the paper by Timoshenko [1] (and his earlier paper [2] on the non-linear buckling of bimetallic curvilinear strips), which dealt with the snapping of a shallow hinged bar under transverse pressure and the determination in explicit form of its upper and lower critical loads, enabled one to look differently on the formulation of the problem of the loss of stability of shells which had existed up to now and to understand the need to employ non-linear equations in its investigation. Moreover, Timoshenko in his paper drew attention to the possibility of extending his results to shallow shells. It would not be an exaggeration to say that Timoshenko's model actually promoted the development of the non-linear theory of shells. Here, it is also worth recalling the fundamental papers of Bubnov [3, 4] on the non-linear behaviour of an infinitely long cylindrical panel under transverse pressure. Timoshenko's bar model has been used in a well-founded manner [5] to analyse the non-linear, axisymmetric behaviour of shallow spherical shells (Fig. 1). However, it was only the publication by Marguerre [6] of the differential equations for thin, elastic, shallow shells for finite flexures, which are a natural extension of the Bubnov–Föppl–Karman equations [3, 4, 7, 8], that enabled us to have a classical, compact system of equations for describing the non-linear deformation of a shell. A a result, it became possible to take account of non-linearity during the deformation of a shell and to obtain an analytic description of its snapping and of its postbuckling behaviour. This possibility was used [9] to solve the Marguerre equations in the case of a shallow, continuous, spherical dome under uniform transverse pressure by the Bubnov method with a single parameter representation of the deflection function and to analyse the axisymmetric, non-linear behaviour for four forms of boundary conditions. A system of differential equations for the finite flexures of shallow shells, which is more accurate compared with Marguerre's classical equations, was subsequently derived by Reissner [10].

A computerized analysis of the behaviour of shallow spherical domes, based on the Marguerre and Reissner equations, has been given in a number of papers [11–16].

These periods in the development of the theory and practice of the design of spherical shells have been described in detail in [17–19] and in [20, 21].

Bach [22] was apparently the first to carry-out an experimental investigation of the behaviour of spherical shells. He discovered that, under a certain external pressure, a spherical shell proves to be unstable and dents appear in it. Much later (in 1939), Boley and Sechler (see [5]) carried out a painstaking experiment with a copper hemisphere, manufactured to a high precision, and established that the critical

†*Prikl. Mat. Mekh.* Vol. 66, No. 4, pp. 621–634, 2002.

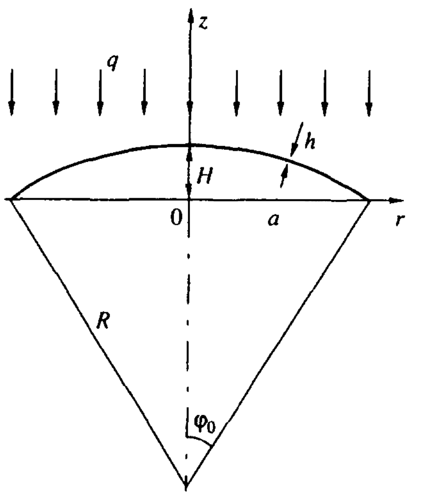

Fig. 1

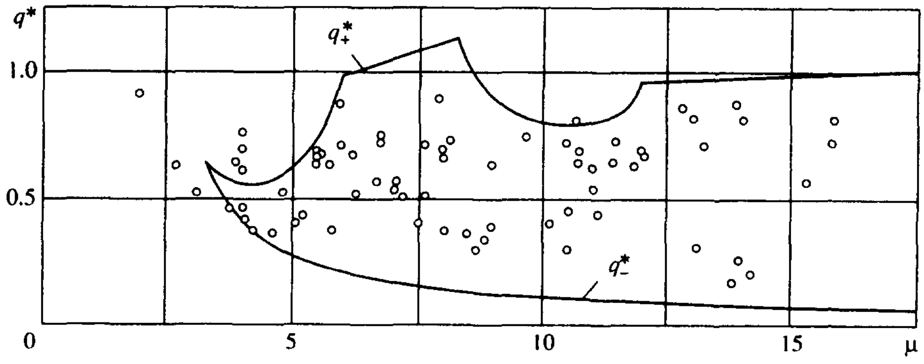

Fig. 2

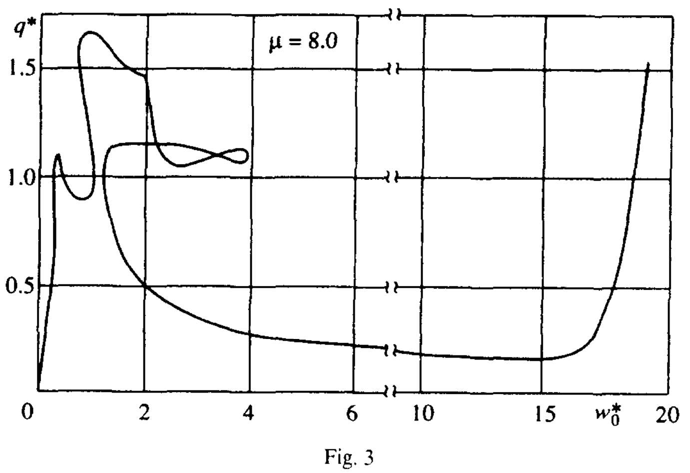

Fig. 3

experimental pressure is four times less than the theoretical value corresponding to the linear theory of the stability of shells (Zoeley's formula). Similar investigations of the behaviour of shallow spherical domes under the uniform transverse pressure were subsequently carried out by a number of researchers [23–30]. A detailed discussion of the work of these and many other investigators has been given in [31].

A comparison of the experimentally and theoretically obtained values of the critical loads of shallow spherical domes showed that there is considerable disagreement between them. This can be seen in

Fig. 2 which is taken from [31]: the dependence of the upper and lower critical loads for an axisymmetrically deforming, shallow spherical dome, which is rigidly clamped along its boundary, on its wall-thinness parameter, which is mainly defined as the ratio of the radius of curvature of the shell to the thickness of its wall, is represented by the solid lines. These are theoretical results obtained by different researchers mainly by solving Marguerre's equations. The values of the upper critical load, taken from experimental papers of the investigators mentioned above, are represented by the small open circles.

This disagreement between the results is associated both with the experimental conditions and with the special features of the mathematical model of a shell which is used. In the first place, neglect of initial irregularities in the shape of a shell and the initial stresses in it, the non-ideality of the loading conditions of the shell and its fixing around its boundary, the inhomogeneity of the properties of the shell material, the asymmetry of it deformation, etc. are referred to here (see [31]). However, as was pointed out in [31], attempts to take account in the calculations of these special features of an actual spherical dome and the methods used in its loading and fixing have not been successful. To this day, there is no set of parameters of a mathematical model of a shell, based on the Marguerre and Reissner equations, which would make it possible to obtain the whole spectrum of experimentally found values of the upper critical loading using a small variation of above parameters.

An attempt to solve the complete problem of the snapping of a shallow spherical dome under the uniform transverse pressure and thereby to confirm its high sensitivity to the above-mentioned imperfections was one of the forms of the solution of this problem. Using the example of an ideal shell, such an attempt has been made by many investigators ([32–36], etc.). However, only Mescall [37] was successful in completely solving this problem. The trajectory of the loading by a uniform transverse pressure of a shallow spherical dome which is rigidly clamped along its boundary [37] is shown in Fig. 3: q^* is the dimensionless radial pressure and w_0^* is the relative deflection of the middle surface at the vertex of the dome. After the publication of [37], no one has succeeded in completely reproducing the process of the postbuckling deformation of a dome, and papers by Mescall himself did not follow. The problem of the postbuckling behaviour of a dome therefore remains unexplained to the end.

In the light of the foregoing discussion, the aim of this paper is to solve the complete problem of the geometrically non-linear deformation of a shallow spherical dome, to carry out a parametric analysis of its deformation and to refine the dependence of the critical loads, corresponding to the limit points of the loading trajectories, on the wall-thinness parameter.

1. THE MATHEMATICAL MODEL OF A DOME

The Marguerre differential equations are the most suitable for describing finite, axisymmetric deflections of an elastic, shallow, spherical dome loaded with a uniform transverse pressure q. In mixed form, they are

$$\nabla^2\nabla^2 F + \frac{Eh}{R}\nabla^2 w + \frac{Eh}{2}\mathbf{N}_2(w,w) = 0$$

$$D\nabla^2\nabla^2 w - \frac{1}{R}\nabla^2 F - \mathbf{N}_2(F,w) = -q; \qquad 0 \leqslant r \leqslant a \tag{1.1}$$

Here ∇^2 is the Laplace operation, N_2 is a non-linear second-order differential operator

$$(\nabla^2\xi = \xi'' + \xi'/r, \quad N_2(\xi,\zeta) = (\zeta''\xi' + \zeta'\xi'')/r, \quad D = Eh^3/[12(1-\nu^2)])$$

a prime denotes a derivative with respect to the radial coordinate r, w is the deflection of the shell, F is the Airy stress function, which is connected with the specific normal forces by the following relations.

$$N_{rr} = F'/r, \quad N_{\theta\theta} = F''$$

R is the radius of curvature of the dome, E is the modulus of elasticity of its material, h is the thickness of its wall, D is its cylindrical stiffness and ν is Poisson's ratio of the dome material.

In the case when the dome is rigidly-clamped along its boundary, these equations must be supplemented with the boundary conditions

$$u = \vartheta_r = Q_r^0 = 0 \quad \text{when } r = 0; \qquad u = \vartheta_r = w = 0 \quad \text{when } r = a \tag{1.2}$$

where u are the radial displacements of the points of the middle surface of the dome, ϑ_r is the angle of rotation of the normal to the middle surface of the dome in a radial direction and Q_r^0 is the generalized transverse radial force

$$Q_r^0 = -D(\nabla^2 w)' + N_{rr}\vartheta_r$$

Marguerre's equations are the differential analogue of the Lagrange equilibrium equation

$$\delta(\Pi - A) = 0 \tag{1.3}$$

in which Π is the potential energy of the deformation of the shell and A is the work of the external load

$$\Pi = \frac{1}{2}\int_0^a\int_0^{2\pi}\{B[e_{rr}^2 + 2\nu e_{rr}e_{\theta\theta} + e_{\theta\theta}^2] + D[\varkappa_{rr}^2 + 2\nu\varkappa_{rr}\varkappa_{\theta\theta} + \varkappa_{\theta\theta}^2]\}rdrd\theta, \quad B = Eh/(1-\nu^2) \tag{1.4}$$

$$A = \int_0^a\int_0^{2\pi} qwrdrd\theta$$

Here, e_{rr}, $e_{\theta\theta}$, $\varkappa_{rr}$ and $\varkappa_{\theta\theta}$ are the deformations and the curvatures of the middle surface of the shell

$$e_{rr} = u' - w/R + w'^2/2, \quad e_{\theta\theta} = u/r - w/R, \quad \varkappa_{rr} = -w'', \quad \varkappa_{\theta\theta} = -w'/r$$

It is convenient to seek the solution of the problem of finite deflections of a shallow spherical dome in displacements, represented in the form of functional series (henceforth summation over i, p, q, r, s is carried out from 1 to K everywhere)

$$u^* = \frac{a}{h^2}u = \sum_i U_i u_i(\rho), \quad w^* = \frac{w}{h} = \sum_i W_i w_i(\rho) \tag{1.5}$$

Here U_i and W_i are the required generalized displacements and, starting out from the structure of the equilibrium equation for the dome (1.1) and boundary conditions (1.2) of the problem, we specify the basis functions $u_i(\rho)$ and $w_i(\rho)$, as follows:

$$u_i(\rho) = A_i J_1(\nu_i\rho), \quad w_i(\rho) = C_i[J_0(\omega_i\rho) - b_i I_0(\omega_i\rho)]$$

$$A_i = \frac{\sqrt{2}}{|J_0(\nu_i)|}, \quad C_i = \frac{1}{|J_0(\omega_i)|}, \quad b_i = \frac{J_0(\omega_i)}{I_0(\omega_i)}; \quad i = 1, 2, \ldots, K$$

where J_0 and J_1 are zeroth and first-order Bessel functions of the first kind, I_0 is the modified zeroth-order Bessel function of the first kind, A_i, C_i and b_i are constants, and the parameters ν_i and ω_i are sought as the roots of the following characteristic equations

$$\nu_i{:}\ J_1(\nu) = 0, \quad \omega_i{:}\ J_1(\omega)I_0(\omega) + J_0(\omega)I_1(\omega) = 0; \quad i = 1, 2, \ldots, K$$

Using the Rayleigh–Ritz method, the displacements in the form of (1.5) are substituted into the expressions for the potential energy of deformation of the shallow spherical dome and the work of the external load (1.4). As a result, after integrating, the potential energy of deformation and the work of the external load are represented by the finite sums

$$\Pi = \pi D\left(\frac{h}{a}\right)^2\left[\sum_p(S_{pq}^{01}U_pU_q + S_{pq}^{02}U_pW_q + S_{pq}^{03}W_pW_q) + \right.$$
$$\left. + \sum_{p,q,r}(S_{pqr}^{10}U_pW_qW_r + S_{pqr}^{11}W_pW_qW_r) + \sum_{p,q,r,s}S_{pqrs}^{19}W_pW_qW_rW_s\right] \tag{1.6}$$

$$A = 2\pi Dq^*\left(\frac{h}{a}\right)^2\sum_p Q_pW_p, \quad q^* = \frac{[3(1-\nu^2)]^{1/2}}{2}\frac{qR^2}{Eh^2} \tag{1.7}$$

Here q^* is the dimensionless transverse load, and the coefficients S_{pq}^{01}, S_{pq}^{02}, S_{pq}^{03}, S_{pqr}^{10}, S_{pqr}^{11}, S_{pqrs}^{19}, and Q_p of the generalized displacements are functions of their own subscripts Poisson's ratio and the wall-thinness parameter of the dome

$$\mu = [12(1-\nu^2)]^{1/4}[a^2/(Rh)]^{1/2}$$

The derivation of the equations of equilibrium with respect to the generalized displacements is the next and last stage in the Rayleigh–Ritz method. In order to do this, the potential energy of deformation Π and the work of the external load A, in the form of the finite sums (1.6) and (1.7), are substituted into Lagrange's equation (1.3) where variation with respect to the values of the generalized displacements U_i and W_i is carried out. As a result, a system of non-linear algebraic equations is obtained for determining them, which can be written in the matrix form

$$\mathbf{f}(\mathbf{x}) = 0 \tag{1.8}$$

$$\mathbf{f} = (f_1 f_2 \ldots f_{2K})^T, \qquad \mathbf{x} = (U_1 W_1 \ldots U_K W_K q^*)^T$$

As the vector $\mathbf{f}$, we have in mind a vector composed of the partial derivatives of the total potential energy of deformation of the shell $\Pi - A$ with respect to the displacements U_i and W_i (i = 1, 2,..., K). The vector $\mathbf{x}$, in accordance with the idea of the equality of the variables of the solution, is made up of the generalized displacements to which the dimensionless transverse load is added and its order is determined by the number of terms taken into account in the partial sums (1.5): $N_{\max} = 2K + 1$.

The system of non-linear algebraic equations (1.8) corresponds to a discrete model of a shallow spherical dome of finite deflections and the next stage in solving the problem involves the solution of this system of equations.

The solution of the system of non-linear algebraic equations (1.8), the order of which is assumed to be equal to n here for simplicity, is constructed by the method of continuous prolongation. By analogy with an approach which has been described previously [38], to do this, the system of linear algebraic equations

$$\mathbf{Jq} = \mathbf{b} \tag{1.9}$$

$$\mathbf{J} = \begin{Vmatrix} f_{1,1} & \cdots & f_{1,n} & f_{1,n+1} \\ \cdots & \cdots & \cdots & \cdots \\ f_{n,1} & \cdots & f_{n,n} & f_{n,n+1} \\ f_{1,n+1} & \cdots & f_{n,n+1} & \varepsilon \end{Vmatrix}, \quad \mathbf{q} = \begin{Vmatrix} \varphi_1 \\ \cdots \\ \varphi_n \\ \varphi_{n+1} \end{Vmatrix}, \quad \mathbf{b} = \begin{Vmatrix} 0 \\ \cdots \\ 0 \\ b \end{Vmatrix}$$

is solved at each step with respect to the parameter λ close to the length of the loading trajectory. The elements of the Jacobian are calculated as the partial derivatives of the left-hand sides of the system of non-linear algebraic equation (1.8) with respect to the arguments of the solution, which also includes the loading parameter. The parameter ε of system (1.9) is chosen from the condition that the matrix of this system should be as well-posed as possible, and the parameter b is chosen from the condition for the solution vector $\mathbf{q}$ to be close to a normalized vector: $\|\mathbf{q}\| = 1$. As a result, the vector $\mathbf{q}$ which, from a geometrical point of view, is a tangent vector to the loading trajectory and the so-called prolongation vector, is the vector of the right-hand sides of the normal system of ordinary differential equation

$$d\mathbf{x}/d\lambda = \mathbf{q}(\mathbf{x}) \tag{1.10}$$

the numerical solution of which gives the coordinates of the points of the loading trajectory of the shell.

The method of discrete prolongation [39] is used to compensate for the errors which are accumulated in the components of the vector $\mathbf{x}$ during the numerical solution of the system of prolongation equations (1.10). This is based on Newton's method, implemented for an extended space of variables. In accordance with [39], each iteration of Newton's method is organized by solving a system of linear algebraic equations of the form

$$\mathbf{J}\Delta\mathbf{x} = -\mathbf{f}_0$$

$$\Delta\mathbf{x} = (\Delta x_1 \ldots \Delta x_n \Delta x_{n+1})^T, \qquad \mathbf{f}_0 = (f_1 \ldots f_n 0)^T$$

which enables one to refine the solution vector $\mathbf{x}$ at any regular point of the loading trajectory, including its limit points.

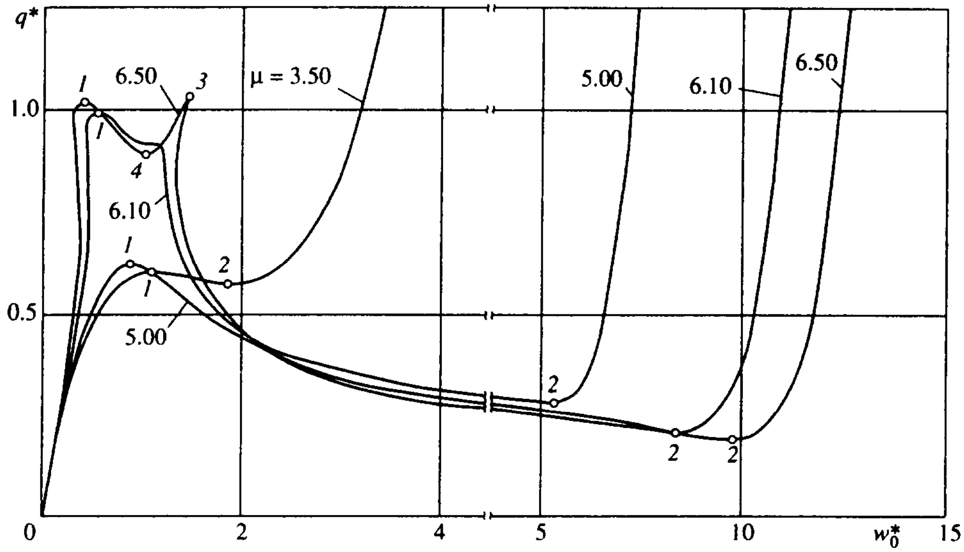

Fig. 4

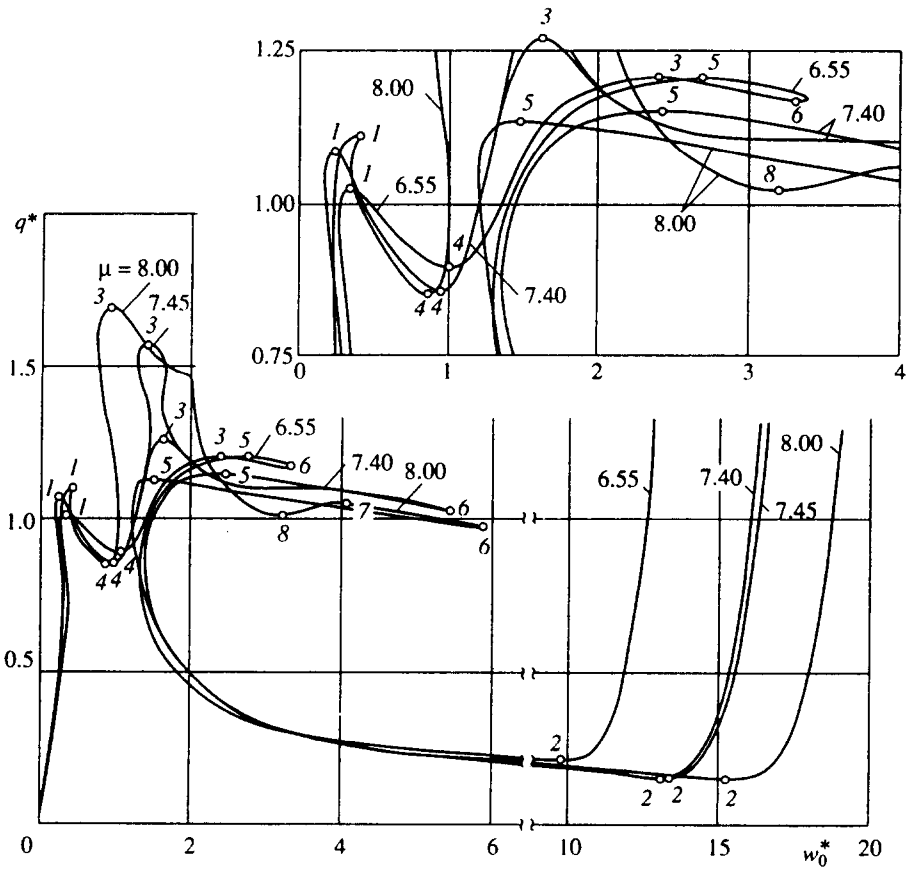

Fig. 5

2. THE EFFECT OF THE WALL-THINNESS PARAMETER ON THE FORM OF THE LOADING TRAJECTORY

If we ignore Poisson's ratio ($\nu \approx 0.3$), which only varies slightly in the case of metals, the wall-thinness parameter μ is practically the only parameter of a shallow spherical shell. It is mainly determined by the apex angle φ_0 and its relative thickness h/R. The thicker the shell wall and the greater its apex angle, the greater the wall-thinness parameter μ. If account is taken of the fact that, in the case of shallow spherical shells, the apex angle does not exceed 22°, then, for the range of relative thicknesses of thin shells $h/R = 1/20\ldots1/200$, the limits of variation of the wall-thinness parameter are found to be $\mu = 0$–18.

The effect of this parameter was investigated, taking as an example the deformation characteristics of a shell in the coordinates q^* and w_0^* over a range of values of μ from 3 to 16. The results of this investigation are shown in Figs. 4–8. The limit points, at which the shell, under conditions of axisymmetric deformation, loses stability by snapping, are given the numbers 1, 2, ... The forms of deflection of the dome, which correspond to its stress–strain state at these points are shown in Table 1 and Fig. 9. The dashes in Table 1 denote that, for the value of the wall-thinness parameter μ indicated in the row being considered, the limit point, which is omitted from the given column of the table, does not exist in the loading trajectory.

The first pair limit points 1 and 2, which determine the values of the first upper and lower critical loads, appears on the loading trajectory when $\mu \approx 3.3$. They can be seen in Fig. 4. An increase in the wall-thinness parameter brings about an evolutionary change in the form of the loading trajectory and, when $\mu \approx 6.2$, leads to the appearance of a second pair of limit points (3 and 4) on it. The process by which they are produced is seen by comparing the curves with $\mu = 6.10$ and 6.50 in Fig. 4.

When the wall-thinness parameter is increased further, there is a jump-like increase in the critical loading, which corresponds to the limit point 3 and the appearance of yet another pair of limit points, 5 and 6. Comparison of the curves the $\mu = 6.50$ and 6.55 in Figs 4 and 5 enables us to assume that the loop for $\mu = 6.55$ in Fig. 5 with the points 3, 5 and 6 has existed for values of the wall-thinness parameter of less than 6.55 in a form which is isolated from the main branch, and its appearance in Fig. 5 is caused by its merging with the main branch.

Increasing the wall-thinness parameter from a value of 6.55 up to 7.40 (Fig. 5) only gives rise to an evolutionary change in the loading trajectory but, when $\mu \approx 7.44$ and simultaneously with the generation of a third pair of limit points, 7 and 8, there is again a sharp increase in the critical load, which is determined by the limit point 3. This is obviously also associated with an isolated loop, which has a limit point 3 in Fig. 5 ($\mu = 7.45$), joining the main branch of the loading trajectory.

When the wall-thinness parameter is changed from 7.45 to 8.20 (Figs 5 and 6) an evolutionary change in the loading trajectory is observed, during which the limit point 6 and 7 disappear and, when $\mu \approx 8.25$, the process, described above, of the merging of the isolated loop shown in Fig. 6 occurs. This can be clearly seen by comparing the curves for $\mu = 8.20$ and 8.35 in Fig. 6.

The next qualitative change in the loading trajectory occurs when $\mu \approx 8.36$. In Fig. 7, there are no loops in the main branch when $\mu = 8.36$. This may only mean that the loops with the limit points 3, 4, 8, 9 and 10 have become detached from it and the transition of this loop into a class of isolated loops. This assumption is confirmed by the behaviour of the limit points 1 and 5. A comparison of Figs 5 and 6 shows the continuous convergence of these points which, when $\mu \approx 8.36$, leads, to all appearance, to their merging.

A further increase in the wall-thinness parameter from 8.36 up to 15.00 repeats the changes in the loading trajectory of a spherical dome described above for $\mu = 3.30$–8.36. The corresponding curves are shown in Figs 7 and 8. Here also, an evolutionary change (see the curves with $\mu = 8.36$–12.80 and $\mu = 12.90$–14.90) and a jump-like change (see the curves with $\mu = 12.80$ and 12.90) of the deformation curves occurs together with the generation of limit points (see the curves with $\mu = 12.00$ and 12.20 and with $\mu = 14.00$ and 14.90) and, also, the joining (see the curves with $\mu = 12.80$ and 12.90) and the detachment of loops as the wall-thinness parameter is increased from 14.90 up to 15.00.

The dependence of the critical loads, corresponding to the limit points 1–12 of the loading trajectory shown in Figs 4–8, is shown in Fig. 10. It is a many-valued curve, the main part of which (branches 1 and 2) describes the upper and lower critical loads (the loads of the limit points 1 and 2) and is identical to the known curve (see Fig. 2). The additional branches 3–12 of this curve show the generation and disappearance of limit points of higher orders 3–12 and the joining and detachment of loops from the main branch of the loading trajectory. Some of them, for example, branches 4 and 6, describe smaller values of the critical loads than those which are characteristic of branch 1. Under actual conditions of the deformation of a shallow spherical dome, these critical states naturally cannot be realized. Their limit points lie in unstable segments of the loading trajectory of the dome and it is impossible to reach them under natural deformation conditions. However, the fact that the critical state of a dome, corresponding to the limit point 4 (see Fig. 5, $\mu = 8.00$, for example), is located sufficiently close to a critical state that corresponds to the first upper critical load, which is entirely realizable in an actual loading process, may turn out to be useful in calculating the deformation of a dome when an initial

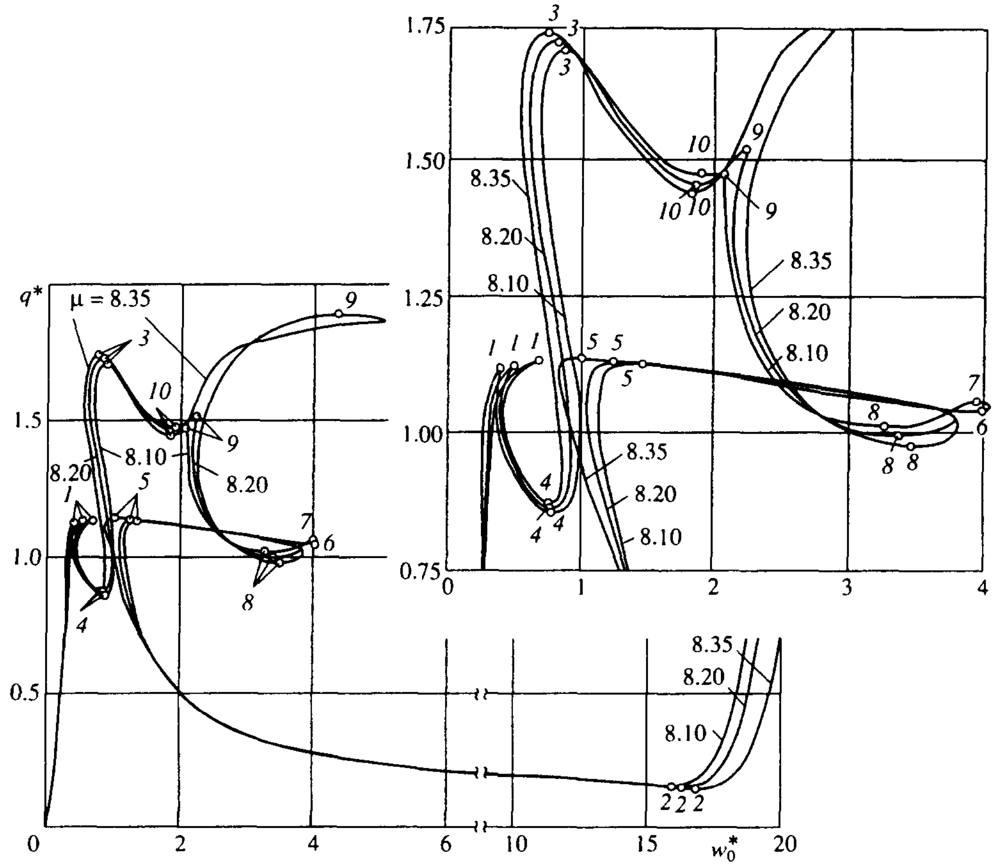

Fig. 6

imperfections in its shape increase. At the same time, consideration of the forms of deflection of the dome (see Table 1, μ = 6.50–8.35), corresponding to the limit points 1 and 4, reveals their steady character. The forms of deflection do not change qualitatively when there is a substantial change in the wall-thinness parameter. It may therefore be assumed that the introduction of an initial imperfection, which is proportional to the form of its deflection corresponding to the limit point 4, into the calculation of the deformation of a dome may appreciably reduce the value of the first upper critical load and, to some extent, reduce the disagreement between the theoretical and experimental data.

3. THE ACCURACY OF THE DETERMINATION OF THE CRITICAL LOADS

The accuracy with which the loading trajectory of a spherical dome and its critical loads can be determined is governed by three facts.

First, the adequacy of the mathematical model in describing the actual phenomena of its non-linear deformation. Under conditions of elastic deformation of a dome, Marguerre's equations for shallow shells of finite deflection, which are used in this calculation as the mathematical model, are assumed to be quite accurate. Attempts have been made to refine them but the admissibility of these equations has never been in doubt. Here, Kirchoff's square law for representing the deformations of its middle surface and the assumption that it is shallow are sources of error when solving the problem of describing the deformation of the shell. Judging from estimates [40, 41], these errors for deflections of a shell, of less than ten thicknesses and shells with an apex angle not greater than 22°, do not exceed 2–5%.

Second, the accuracy of the discretization method, that is, of the Rayleigh–Ritz method, has an effect on the accuracy with which the loading trajectory of a spherical dome can be constructed. The accuracy is determined by the accuracy of the approximation of the displacements of the shell, which can only be elucidated by means of a numerical experiment. With this aim, the values of the critical loads, corresponding to their limit points, were calculated using a different number of terms K in the sums (1.5), approximating the displacements for two shells with wall-thinness parameters μ = 8.35 and μ = 14.90, the trajectories of which (see Figs 6 and 8) are the most branched. The results of these

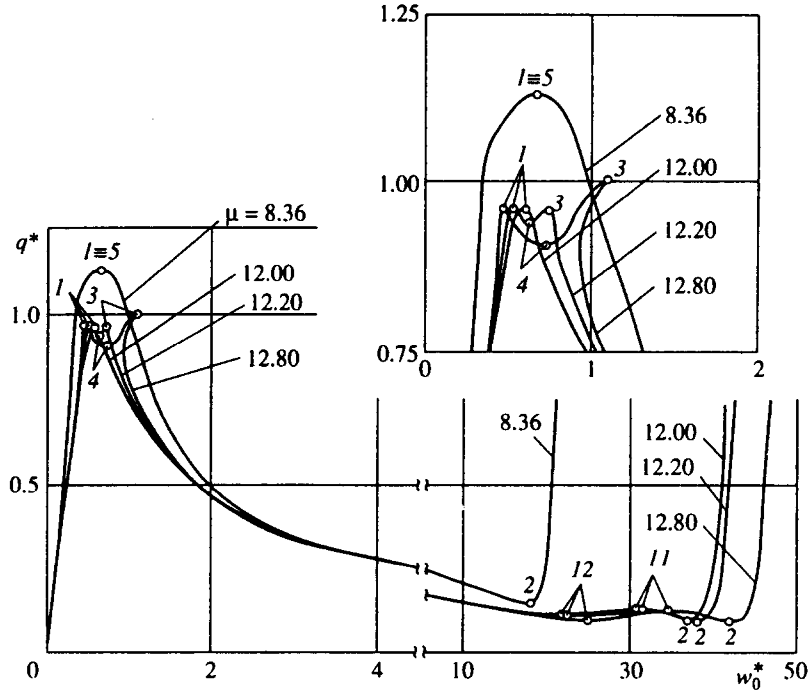

Fig. 7

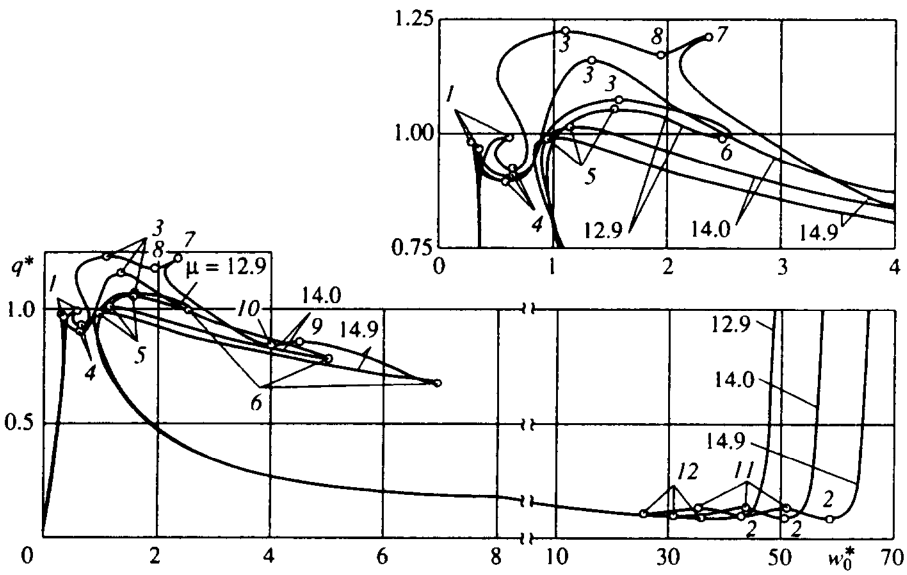

Fig. 8

calculations are shown in Table 2 for certain limit points of the loading trajectory. The dashes in this table mean that, for the value of the number of terms K indicated in the row under consideration, the limit point which is left out of the column of the table does not exist in the loading trajectory. The data in Table 2 show that fourteen terms in the sums which are used are quite sufficient to determine the critical loads of a spherical dome with a wall-thinness parameter $\mu = 8.35$ with an accuracy up to four significant figures and, in the case of a dome with a wall-thinness parameter $\mu = 14.90$, with an accuracy up to three significant figures. In the first case, the relative error in determining the critical loads does not exceed 0.01% and, in the second case, 0.1%.

The third fact which determines the accuracy with which the critical loads of a spherical dome can be found is the accuracy of the solution of the system of non-linear algebraic equilibrium equations (1.8) by the method of prolongation. The computational basis in implementing this method is Simpson's

Table 1

μ	Number of a Limit Point								
	1	3	4	5	6	7	8	9	10
3.50	*B*	–	–	–	–	–	–	–	–
5.00	*A*	–	–	–	–	–	–	–	–
6.10	*C*	–	–	–	–	–	–	–	–
6.50	*C*	*A*	*C*	–	–	–	–	–	–
6.55	*C*	*D*	*C*	*D*	*D*	–	–	–	–
7.40	*C*	*A*	*C*	*D*	*D*	*D*	*D*	–	–
7.45	*C*	*E*	*C*	*D*	*D*	*D*	*D*	–	–
8.00	*C*	*E*	*C*	*D*	*D*	*D*	*D*	–	–
8.10	*C*	*E*	*C*	*D*	*D*	*D*	*D*	*A*	*A*
8.20	*C*	*E*	*C*	*D*	–	–	*D*	*A*	*C*
8.35	*C*	*E*	*C*	*C*	–	–	*D*	*F*	*C*
8.36	*C*	*E*	–	–	–	–	–	–	–

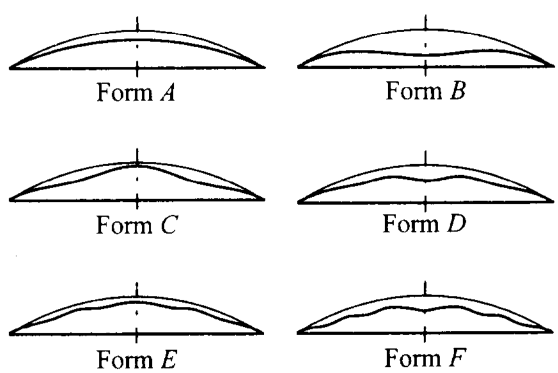

Fig. 9

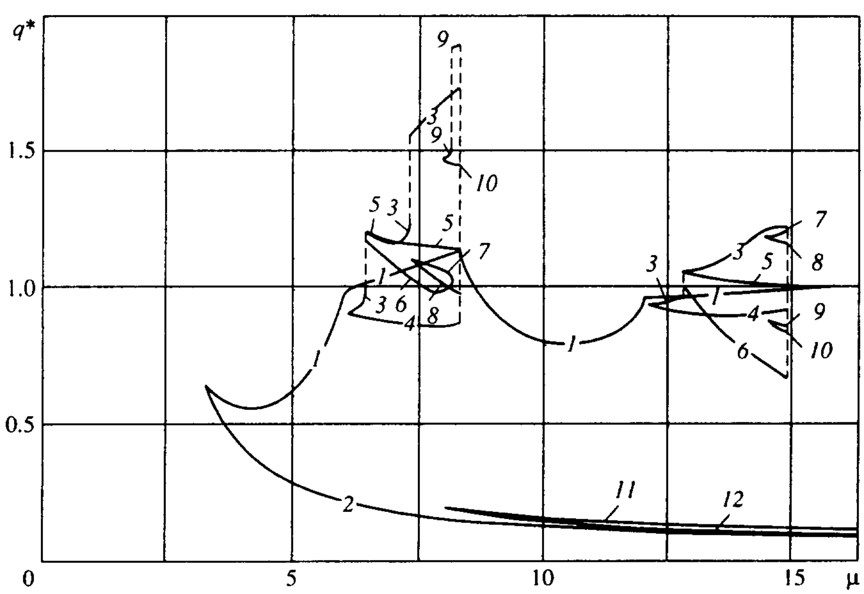

Fig. 10

Table 2

K	q_1	q_2	q_3	q_4	q_5	q_8
			$\mu = 8.35$			
7	1.117	0.1562	–	–	–	–
8	1.131	0.1487	1.810	0.8674	1.144	0.9534
9	1.129	0.1470	1.830	0.8686	1.135	0.9805
10	1.130	0.1471	1.844	0.8681	1.134	0.9750
11	1.130	0.1471	1.737	0.8682	1.134	0.9754
12	1.130	0.1472	1.744	0.8682	1.135	0.9755
13	1.130	0.1472	1.741	0.8682	1.134	0.9754
14	1.130	0.1472	1.741	0.8683	1.134	0.9754
			$\mu = 14.90$			
7	1.138	–0.2931	2.149	0.9637	–	–
8	1.014	–0.1549	1.239	0.6603	–	–
9	0.997	–0.0547	1.214	0.7773	–	–
10	0.998	0.0188	1.221	0.8624	0.9993	1.183
11	0.993	0.0656	1.225	0.9098	0.9949	1.179
12	0.993	0.0899	1.230	0.8995	0.9949	1.180
13	0.992	0.0878	1.214	0.9141	0.9939	1.171
14	0.992	0.0879	1.217	0.9144	0.9938	1.166

formula for evaluating definite integrals, Gauss, method for solving systems of linear algebraic equations, Newton's method for solving systems of non-linear algebraic equations and the Kutta–Merson method for solving the Cauchy problem. The errors in using Simpson's formula and the Kutta–Merson method to solve the problem are controlled by a double recalculation using the Runge rule and do not exceed, with respect to their relative value, 10^{-6} for each integral in Simpson's formula and for the norm of the solution in the Kutta–Merson method. The vector of the discrepancies in Newton's method in the last iteration does not exceed, with respect to its norm, a value equal to 10^{-5} of the norm of the solution. Gauss' method is used in the calculations in a version which makes a choice of the leading element at each step of a straight path. Its error is not monitored. However, in calculations with a seven-place digit grid, there is an estimate for it with respect to the norm of the solution of $\varepsilon \sim 10^{-6}n$, where n is the order of the system. In this investigation, the order of the system did not exceed thirty and the relative error of Gauss' method was therefore a quantity not exceeding 10^{-4}.

Summing up what has been said, it can be asserted that this solution of the problem of a geometrically non-linear deformation of a shallow, elastic, spherical dome has been obtained with a relative error not exceeding 5%.

4. CONCLUSION

The variability of the deformation curve of a shallow, spherical dome over a range of relative thicknesses of its wall $h/R \approx 1/20$–$1/200$ has an evolutionary and jump-like character. This is associated with the generation of limit points on the loading trajectory, and their merging and subsequent disappearance, and, also, the merging joining of isolated loops with the main loop of the loading trajectory and the detachment of them from it. These phenomena occur frequently in the case of a quite small change in the wall-thinness parameter of the dome, which confirms the assumption regarding its high sensitivity to deviations from an ideal shape. The dependence of the critical loads, corresponding to the limit points of the loading trajectory, on the wall-thinness parameter of the shell is described by a many-valued curve, the main part of which is identical to the known curve, and the additional branches show the generation and disappearance of limit points of higher orders. Several of them describe the values of critical loads which are less than the upper critical load. This fact may turn out to be useful when calculating the deformation of a dome taking account of initial imperfections in its shape.

This research was supported by the Competition Centre for Basic Natural Science.

REFERENCES

1 TIMOSHENKO, S., Buckling of flat curved bars and slightly curved plates. *J. Appl. Mech.*, 1935, **2**, 1, 17–20.
2. TIMOSHENKO, S., Analysis of bi-metal thermostats. *J. Optical Soc. of Am. Rev. of Sci. Instruments*, 1925, **11**, 3, 233–255.
3. BUBNOV, I. G., Stresses in the cladding of vessels from the pressure of water, *Morskoi Sb.*, 1902, **311**, 8, 117–141; **312**, 9, 111–139, 312; 10, 119–138; **313**, 12, 107–130.
4. BOOBNOFF, I. G., On the stresses in a ship's bottom plating due to water pressure. *Trans. Inst. Naval Arch.*, 1902, **44**, March, 15–46; 51–52.
5. KARMAN, Th. Von. and TSIEN, S., The buckling of spherical shells by external pressure. *J. Aeronaut. Sci.*, 1939, **7**, 2, 43–50.
6. MARGUERRE, K., Zur Theories der gerkrümmten Platte großer Formänderung. *Proc. 5th Int. Congr. Appl. Mech.*, Cambridge, Massachusetts, 1938, Wiley, New York, 1939. 93–101.
7. FÖPPL, A., *Vorlesungen über technische Mechanik*, vol. 5, *Die wichtigsten Lehren der höheren Elastizitätstheorie*. B. G. Teubner, Leipzig, 1907.
8. KARMAN, Th., Festigkeitsprobleme im Maschinenbau. *Encyklopädie der mathematischen Wissenschaften*, B. G. Teubner, Leipzig, 1910, vol. 4, 348–352.
9. FEODOS'YEV, V. I., Analysis of a buckled membrane, *Prikl. Mat. 3 Mekh.*, 1946, **10**, 2, 295–300.
10. REISSNER E., On axisymmetrical deformation of thin shells of revolution. *Proc. 3rd Sympos. Appl. Math.* McGraw-Hill, New York, 1950. Vol. 3, 27–52.
11. REISS, E. L., On the nonlinear buckling of shallow spherical domes. *J. Aeronaut. Sci.*, 1956, **23**, 10., 973–975.
12. SIMONS, R. M., A power series solution of the nonlinear equations for axi-symmetrical bending of shallow spherical shells. *J. Math. and Phys.*, 1956, **35**, 2, 164–176.
13. REISS, E. L., GREENBERG, H. J. and KELLER, H. B., Nonlinear deflections of shallow spherical shells. *J. Aeronaut. Sci.*, 1957, **24**, 7, 533–543.
14. WEINITSCHKE H. J., On the nonlinear theory of shallow spherical shells. *J. Soc. Indust. Appl. Math.*, 1958, **6**, 2, 209–232.
15. ARCHER, R. R., Stability limits for a clamped spherical shell segment under uniform pressure. *Quart. Appl. Math.*, 1958, **15**, 4, 355–366.
16. BUDIANSKY, B., Buckling of clamped shallow spherical shells. *Proc. Symp. on the Theory of Thin Elastic Shells*, Delft, 1959. North-Holland, Amsterdam. 1960, 64–94.
17. TIMOSHENKO, S. and WOINOWSKY-KRIEGER, S., *Theory of plates and shells*, McGraw-Hill, New York, 1959.
18. VOL'MR, A. S., *The Stability of Deformable Systems*. Nauka, Moscow, 1967.
19. GROGOLYUK, E. I. and KABANOV, V. V., *The Stability of Shells*. Nauka, Moscow, 1978.
20. KARMAN, Th. Von. and KERR, A. D., Instability of spherical shells subjected to external pressure. *Topics Appl. Mech.*, Amsterdam, 1965, 1–22.
21. SUNAGAWA MEGUMI and KUMAI NORI, The resistance of structures to dynamic loading. *J. Jap. Soc. Aeronaut. and Space Sci.*, 1970, **18**, 195, 154–166.
22. BACH, C., Die Widerschtandfähigkeit kugelförmiger Wandung gegenüber äusserem über-druck. *Z. Vereines deutscher Ingenieur*, 1902, **46**, 10, 333–341.
23. TSIEN, H.-S., A theory for the buckling of thin shells. *J. Aeronaut. Sci.*, 1942, **9**, 10, 373–384.
24. KLÖPPEL, K., and JUNGBLUTH, O., Beitrag zum Durchschlagsproblem dünnwandiger Kugelschalen (Versuche und Bemessungsformeln). *Der Stahlbau.*, 1953, **22**, 6, 121–130.
25. KAPLAN A., and FUNG, Y. C., A nonlinear theory of bending and buckling of thin shallow spherical shells. NACA Techn. Notes, 1954, 3212.
26. HOMEWOOD, R. H., BRINE, A. C. and JOHNSON, A. E., Experimental investigation of the buckling instability of monocoque shells. *Proc. Soc. Expt. Stress Analysis.*, New York, 1963, **18**, 1, 88–96.
27. KRENZKE M. A. and KIERNAN, T. J., Elastic stability of near perfect shallow spherical shells. *AIAA Journal*. 1963, **1**, 12, 2855–2857.
28. ADAM H. P. and KING, P. A., Experimental investigation of the stability of monocoque domes subjected to external pressure. *Experi. Mech.*, 1965, **5**, 10, 313–320.
29. SUNAKAWA, M. and ICHIDA, K., A high precision experiment on the buckling of spherical caps subjected to external pressure. *Report Inst. Space and Aeronaut. Sci. Univ. Tokyo*, Tokyo, 1974, **3**, 508, 87–121.
30. GALLETLY, G. D., On the buckling of shallow spherical caps subjected to uniform external pressure. *AIAA J.*, 1976, **14**, 9, 1331–1333.
31. GRIGOLYUK, E. I. and MAMAI, V. I., *The Mechanics of the Deformation of Spherical Shells*. Izd. Moskovsk. Gos. Univ., Moscow, 1983.
32. WEINITSCHKE, H., On the stability problem for shallow spherical shells. *J. Math. and Phys.*, 1960, **38**, 4., 209–231.
33. THURSTON, G. A., A numerical solution of the nonlinear equations for axisymmetric bending of shallow spherical shells. *Trans. ASME. Ser. E. J. Appl. Mech.*, 1961, **28**, 4, 557–562.
34. SHIL'KRUT, D. I., SHEVANDRONOV, N. V., MORAR, V. P. and MAKSIMOV, Yu. A., *Solution of Problems of the Non-Linear Theory of Shells on Analogue Computers*. Izd. Akad. Nauk MoldSSR, Kishinev, 1969.
35. BAUER, L., REISS, E. L. and KELLER, H. B., Axisymmetric buckling of rigidly clamped hemispherical shells. *Int. J. Non-Linear Mech.*, 1973, **8**, 1, 31–39.
36. VALISHVILI, N. V., *Methods of Designing Shells of Revolution using a Digital Computer*. Mashinostroyeniye, Moscow, 1976.
37. MESCALL, J., Numerical solutions of nonlinear equations for shells of revolution. *AIAA Journal*, 1966, **4**, 11, 2041–2043.
38. GRIGOLYUK, E. I. and LOPANITSYN, Ye. A., The method of continuous prolongation with respect to a parameter. *Dokl. Ross. Akad. Nauk*, 1994, **335**, 5, 582–585.
39. GRIGOLYUK, E. I. and LOPANITSYN, Ye. A., A Modification of the method of discrete prolongation with respect to a parameter. *Zh Prikl. Mekh. Tekh. Fiz.*, 1990, 5, 95–99.
40. VLASOV, V. Z., *The General Theory of Shells and its Application in Technology*. Gostekhizdat, Moscow and Leningrad, 1949.
41. MUSHTARI, Kh. M. and GALIMOV, K. Z., *The Non-linear Theory of Elastic Shells*. Tatknigoizd at, Kazan, 1957.

Translated by E.L.S.